

Simulations of antihydrogen formation in a nested Penning trap

S. Jonsell, D. P. van der Werf and M. Charlton

Department of Physics, Swansea University, Swansea SA2 8PP, United Kingdom

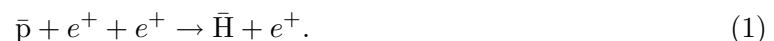
E-mail: b.s.jonsell@swansea.ac.uk

Abstract. We have simulated the formation of antihydrogen through three-body recombination using classical trajectories of antiprotons and positrons. The simulations include several effects which are important in current antihydrogen experiments: the full motion of the antiproton repeatedly passing into and out of the positron plasma, the energy loss of antiprotons due to the interaction with the positron plasma, and the field-ionization of antihydrogen en route from the plasma to the detector. We find that whereas the overall simulated rate of formation of antihydrogen has a density dependence close to n_e^2 , the rate of antihydrogen detection follows a power law less than 2. The difference is due to the effect of density dependent field ionization.

1. Introduction

Antihydrogen can be used for precision tests of fundamental matter-antimatter symmetries. This is the goal of a number of experiments using the Antiproton Decelerator (AD) at CERN. Here the first experiments, ATHENA [1] and ATRAP [2], managed to form cold antihydrogen in 2002. The efforts to trap and cool antihydrogen continue. Presently, two experiments, ALPHA [3] and ATRAP [4], are working towards the goal of trapping antihydrogen for future spectroscopic tests of the CPT symmetry. There are also new experiments underway from the ASACUSA and AEGIS collaborations [5]. Along with the experimental efforts there has been a lot of theoretical work trying to interpret results and suggest new strategies. For a recent review see Ref. [6]. A good understanding of the formation process is necessary to guide the experiments. This is the motivation for the simulations of antihydrogen formation presented in this paper.

In the ATHENA, ALPHA and ATRAP experiments antihydrogen is formed from antiprotons and positrons trapped together in a nested Penning trap. At the relevant temperature and density the most prominent formation mechanism is three-body collisions,



Through this process weakly bound Rydberg states of antihydrogen are created. To stabilize the anti-atom its binding energy has to be increased through further collisions. However, more often the anti-atom will be ionized again, either through collisions with positrons or by the electric field present in the trap. An alternative formation mechanism is the radiative process,



This process will yield more tightly bound antihydrogen, and is therefore interesting even though it is likely to be much more rare. In our present simulations the radiative process is not included.

Table 1. Radii and lengths of positrons plasmas for different plasma densities n_e and particle numbers N_e . In all cases $T_e = 15$ K.

n_e (m^{-3})	N_e	radius (mm)	length (mm)
5×10^{13}	1.4×10^7	2.87	16.52
1×10^{14}	2.8×10^7	2.41	23.56
2×10^{14}	5.6×10^7	2.06	32.16
5×10^{14}	1.4×10^8	1.70	51.18
1×10^{15}	1.2×10^8	1.11	51.75

2. Method

We simulate the experiments by calculating trajectories of antiprotons in the nested Penning trap. The simulations start with the initialization of antiprotons moving along the axis of the trap with some pre-set kinetic energy, in most cases 2 eV. The path of the antiprotons back and forth through the positron plasma is then followed, with the probability of collision with a positron calculated in each time step. A collision is defined as an event when a positron comes within a box with side length $n_e^{-1/3}$ (where n_e is the density of the positron plasma) centered at the antiproton. As long as the positron stays inside this box its trajectory is calculated, along with that of the antiproton and those of any positron already present or later entering the box. The operational definition of an antihydrogen atom is a state with one positron inside this box. The interaction between the antiproton and positrons outside the box is included as an energy loss of a charged particle in an oppositely charged and magnetized medium [7]. The simulation ends when an antiproton in the form of antihydrogen reaches the detectors surrounding the trap or when it is trapped outside the positron plasma and therefore lost for antihydrogen formation. Such trapping of antiprotons is the result of field ionization of loosely bound antihydrogen by the electric fields in the region between the positron plasma and the detectors. More details can be found in [8].

The calculations are purely classical, using an adaptive step-size Runge-Kutta algorithm to integrate Newton's equation of motion. The force on the antiproton and any positrons present include their mutual Coulomb interaction, along with the force from the external electric and magnetic fields. The magnetic field is constant and directed along the axis of the trap, thus providing the radial confinement of the particles. In most simulations, we set the magnetic field to $B = 3$ T, which is the value used by the ATHENA experiment [1]. The electric field arises from the cylindrical electrodes surrounding the trap and from the space charge of the positron plasma. The electric field and the density distribution of the positrons are determined by solving Poisson's equation self-consistently at the appropriate positron temperature, in the simulations presented here set to $T_e = 15$ K [9]. Other input parameters to the calculation of the electric fields are the peak density of the positron plasma and the number of positrons. We used plasma densities between $5 \times 10^{13} \text{ m}^{-3}$ and 10^{15} m^{-3} and positron numbers between 1.4×10^7 and 1.4×10^8 . This corresponds to typical experimental parameters, for instance in [1] the plasma density was $2.5 \times 10^{14} \text{ m}^{-3}$ and the positron number 7×10^7 . The plasma parameters are summarised in Table 1. The number of antiprotons in the experiments, typically a few 1000 per mixing experiment, is small enough to justify the neglect of antiproton-antiproton interactions.

From our simulations we can extract distributions of velocities, binding energies etc. of the detected antihydrogen. We can also extract spatial and time distributions of antihydrogen formation. Moreover, we can improve our understanding of the formation process by extracting properties of the antiprotons/antihydrogen at intermediate times before their detection.

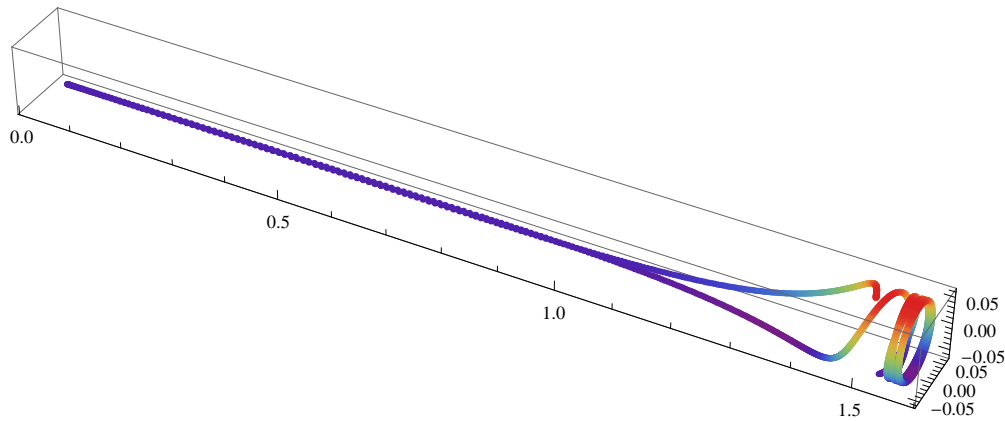


Figure 1. Part of an antiproton trajectory in a nested Penning trap. Inside the positron plasma (to the right) the antiproton follows a helical magnetron motion around the axis of the trap (the radius of the cyclotron motion is too small to be resolved). To the left the antiproton leaves the plasma, is reflected back by a barrier in the electric potential and returns to the positron region. The length scales on the axes are in cm.

3. Formation rates

Antihydrogen formation is a multi-step process which requires time. The final states of the three-body process in eq. (1) are too loosely bound to have any chance to survive the electric fields between the plasma and the detector. The antihydrogen must therefore stabilize by gaining binding energy through repeated collisions with positrons. Such collisions may also have the opposite effect, namely reducing the binding energy or ionizing the antihydrogen. Therefore only a small fraction of the antihydrogen atoms initially formed will eventually leave the plasma, either to be detected or field ionized outside the positron plasma.

The rate of recombination is often described as the rate at which atoms pass a “bottleneck” at a binding energy of a few $k_B T_e$. Atoms with binding energies greater than this bottleneck are very unlikely to be re-ionized. For an antiproton immersed in a plasma with temperature T_e and density n_e , the formation rate has been calculated to be $C(e^2/(4\pi\epsilon_0))^5 m_e^{-1/2} n_e^2 (k_B T_e)^{-9/2}$ (here m_e is the electron mass and the other constants have their usual meaning), where $C = 0.76$ for $B = 0$ [10], $C = 0.11$ for $B = 3$ T [11] and $C = 0.070$ for $B = \infty$ [12].

These rates were derived assuming that the antihydrogen with binding energies above the bottleneck reach a steady state distribution, from which anti-atoms trickle down towards the ground state. This is, however, not a good description of the current antihydrogen experiments. As was pointed out by Robicheaux [13], an important feature of these experiments is that the antiprotons only spend a short time inside the positron plasma. The antiprotons traverse the positron plasma along the axis of the trap. After leaving the plasma they pass a well in the electric potential energy (which for the oppositely charged positrons is a barrier providing their axial confinement, and thus a necessary feature of the experiment), before they are reflected back by a barrier in the electric potential. (An example of part of an antiproton trajectory is shown in Figure 1.) Hence, there will not be time to establish a steady-state distribution, and indeed very few antihydrogen have binding energies greater than the bottleneck energy. Instead, the distribution of binding energies will be a snap-shot taken at the time the antihydrogen leaves the plasma. Most of the antihydrogen will therefore be very loosely bound, and a large fraction will not survive the electric fields between the positron plasma and the detector. Field ionization will usually lead to trapping of the antiprotons outside the positron plasma, and is hence a loss process for antiprotons.

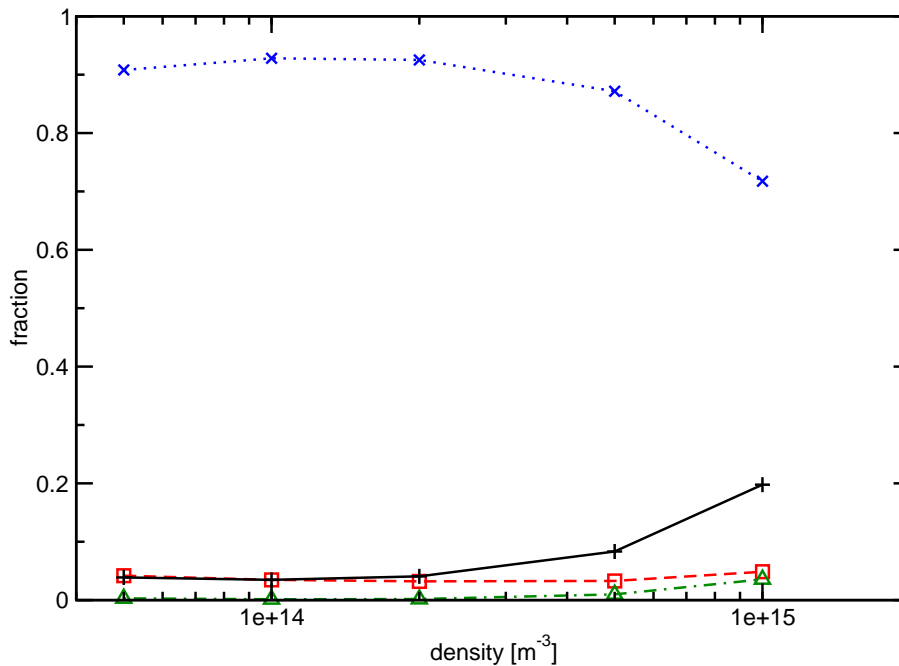


Figure 2. Fraction of antihydrogen atoms formed with a binding energy of at least $k_B T_e$ that re-ionize within the plasma (blue, $\cdots\cdots$, \times), are field ionized outside the plasma leading to loss of the antiproton (black, --- , $+$), survive to the detector (red, --- , \square) or ionized with the antiproton returning to the plasma (green, $\text{-}\cdot\text{---}$, \triangle). The magnetic field was $B = 3$ T and the plasma temperature $T_e = 15$ K.

The relative probabilities of the various possible outcomes for an antihydrogen atom formed in the plasma are shown in Figure 2 as a function of plasma density. Here an antihydrogen atom with kinetic energy from a thermal distribution with temperature $T_e = 15$ K and binding energy greater than $k_B T_e$ was formed at a random position inside the positron plasma. The status of the antiproton as it left the plasma (either as a single particle or inside an antihydrogen atom) was recorded. We find that around 90% of the time the antihydrogen is ionized before it leaves the plasma for most densities. The probability that the antihydrogen survives to the detector is relatively constant, around 3–4% for all densities. The drop in the re-ionization probability at the highest density arises because of repeated formation events in a single pass through the plasma. In fact, at $n_e = 10^{15} \text{ m}^{-3}$ the antiproton on average goes through 5 cycles of antihydrogen formation and re-ionization in a single pass through the plasma.

The effect of field ionization is evident in Figure 3. Here we compare the distribution of binding energies of antihydrogen atoms just after they have left the plasma to the same distribution for antihydrogen reaching the detector. We see that almost all antihydrogen with binding energies less than 50 K, and the majority of those with binding energy between 50 K and 80 K, have been field ionized. This constitutes the majority, about 82%, of the antihydrogen formed. This fraction is density dependent, with a smaller fraction of field-ionized antihydrogen at lower positron densities. Hence, the rate of antihydrogen detection is modified in a density dependent way. This is shown in Figure 4. Here we find that the total formation rate scales with density to a power just below 2, whereas the rate of antihydrogen detection is significantly reduced, scaling as $n_e^{1.67}$.

We are presently working on the temperature dependence of the formation rate. Preliminary

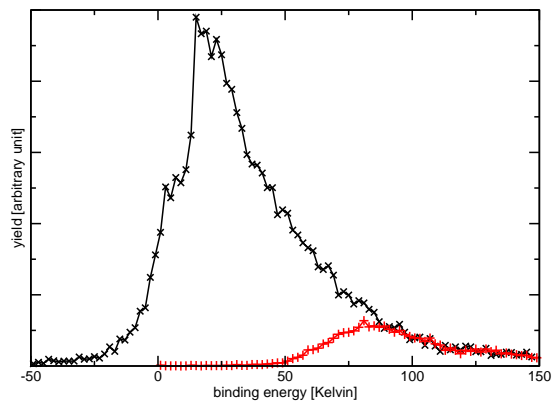


Figure 3. Distribution of binding energies for antihydrogen just after leaving the positron plasma (black, —, ×) and when reaching the detector (red, - - -, +). 18% of the antihydrogens reach the detector. In this simulation $n_e = 10^{15} \text{ m}^{-3}$, $T_e = 15 \text{ K}$, and $B = 3 \text{ T}$. The small number of antihydrogens with negative binding energies are metastable and dissociate before they reach the detector.

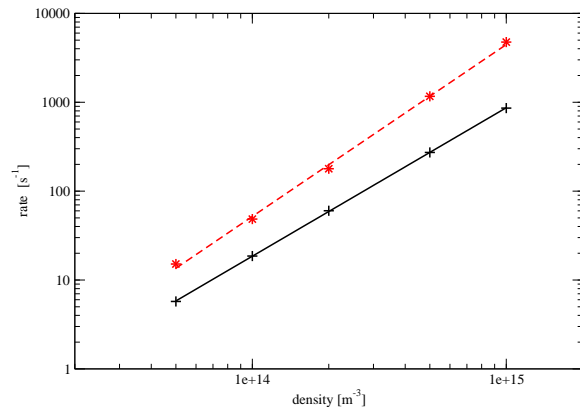


Figure 4. Antihydrogen formation rates as a function of positron density: (black, —, +) rate of antihydrogen detection, (red, - - -, *) total formation rate (including antihydrogen that is field ionized outside the plasma). In this simulation $T_e = 15 \text{ K}$, and $B = 3 \text{ T}$. The solid lines are power-law fits, giving the exponents 1.67 ± 0.01 for detected antihydrogen and 1.93 ± 0.05 for the total rate.

results indicate that the temperature scaling is less steep than the $T_e^{-9/2}$ predicted for the steady-state situation. This is qualitatively in accordance with recent experiments [14].

4. Conclusions

We have studied the dependence of antihydrogen formation rates from three-body recombination on the density of the positron plasma. We find that the short time the antiproton spends in the positron plasma, as pointed out in Ref. [13], along with the field-ionization of loosely bound antihydrogen, has a profound effect on the formation rate. In particular, the antihydrogen detection rate has a weaker density dependence than the n_e^2 one would normally expect for a three-body process.

Other findings will be described in detail in a forthcoming publication [8]. This includes the epithermal nature of antihydrogen formation when the positron density is high, a drift of antiprotons away from the axis of the trap and a mechanism for field-ionization of so-called giant dipole states of antihydrogen.

Acknowledgments

We wish to thank Professor Francis Robicheaux for making his computer programs available and for valuable discussions. We are grateful to the EPSRC (UK) for the support of our work under grants EP/D038707/1, EP/E048951/1, EP/G041938/1 and EP/D069785/1. We also gratefully acknowledge the use of the North West Grid and the UK National Grid Service in carrying out this work.

References

- [1] Amoretti M *et al.* 2002 *Nature* **419** 456
- [2] Gabrielse G *et al.* 2002 *Phys. Rev. Lett.* **89** 213401
- [3] Andresen G *et al.* 2007 *Phys. Rev. Lett.* **98** 023402

- [4] Gabrielse G *et al.* 2007 *Phys. Rev. Lett.* **98** 113002
- [5] See articles in these proceedings.
- [6] Robicheaux F 2008 *J. Phys. B: At. Mol. Opt. Phys.* **41** 192001
- [7] Nersisyan H B, Walter M and Zwicknagel G 2000 *Phys. Rev. E* **61** 7022
- [8] Jonsell S, van der Werf D P, Charlton M and Robicheaux F Accepted for publication by *J. Phys. B: At. Mol. Opt. Phys.*
- [9] Dubin D H E and O'Neil T M 1999 *Rev. Mod. Phys.* **71** 87
- [10] Mansbach P and Keck J 1969 *Phys. Rev.* **181** 275
- [11] Robicheaux F and Hanson J D 2004 *Phys. Rev. A* **69** 010701(R)
- [12] Glinsky M E and O'Neil T M 1991 *Phys. Fluids B* **3** 1279
- [13] Robicheaux F 2004 *Phys. Rev. A* **70** 022510
- [14] Fujiwara M C *et al.* 2008 *Phys. Rev. Lett.* **101** 053401